technologies

MDPI

Article

Field Data Retrieval for Electric Vehicles and Estimating Equivalent Circuit Model Parameters via Particle Swarm Optimization

Syed Adil Sardar [1], Shahzad Iqbal [1], Jeongju Park [2], Sekyung Han [2,*] and Woo Young Kim [1,*]

[1] Faculty of Applied Energy System, Department of Electronics Engineering, Jeju National University, Jeju 63243, Republic of Korea; adilsardar83@stu.jejunu.ac.kr (S.A.S.); shahzadiqbal@stu.jejunu.ac.kr (S.I.)
[2] Department of Electronic and Electrical Engineering, Kyungpook National University, Daegu 41566, Republic of Korea; wjdwn929@naver.com
* Correspondence: skhan@knu.ac.kr (S.H.); semigumi@jejunu.ac.kr (W.Y.K.)

Abstract: Data retrieval techniques are crucial for developing an effective battery management system for an electric vehicle to accurately assess the battery's health and performance by monitoring operating conditions such as voltage, current, time, temperature, and state of charge. This paper proposes an efficient approach to retrieve real-world field data (voltage, current, and time) under running vehicle conditions. In the first step, noise is removed from the field data using a moving-average filter. Then, first- and second-order derivations are applied to the filtered data to determine specific data set conditions. After that, a new approach based on zero-crossing is implemented to retrieve the field data. A second-order Randle circuit (SORC) is utilized in this study to analyze the selected field data. Further, a particle swarm optimization algorithm is adapted to estimate the parameters of the SORC. Our experiments indicate that the relative errors of the equivalent circuit model (ECM) are less than 2% compared to the model voltage and real voltage, which is consistent with the stable parameters of ECM.

Keywords: electric vehicles; data retrieval techniques; equivalent circuit model; battery modeling; optimization algorithms

check for updates

Academic Editor: Valeri Mladenov

Received: 3 January 2025
Revised: 10 February 2025
Accepted: 19 February 2025
Published: 1 March 2025

Citation: Sardar, S.A.; Iqbal, S.; Park, J.; Han, S.; Kim, W.Y. Field Data Retrieval for Electric Vehicles and Estimating Equivalent Circuit Model Parameters via Particle Swarm Optimization. *Technologies* **2025**, *13*, 91. https://doi.org/10.3390/technologies13030091

Copyright: © 2025 by the authors. Licensee MDPI, Basel, Switzerland. This article is an open access article distributed under the terms and conditions of the Creative Commons Attribution (CC BY) license (https://creativecommons.org/licenses/by/4.0/).

1. Introduction

In recent years, rapid advancements in electric vehicle (EV) technology have accelerated due to the high fossil fuel consumption and growing demand for clean energy [1–4]. Electric vehicles rely heavily upon lithium-ion (Li-Ion) batteries, which must be monitored and controlled precisely by a battery management system (BMS) to maintain safety, enhance driving ranges, extend service life, and lower battery costs [4,5]. The key feature of BMSs is the determination of different battery states [6], such as state-of-charge (SoC), state-of-health (SoH) [7,8], and state-of-energy (SoE) [9,10]. Among them, SoC is considered one of the most critical parameters of BMSs, which directly represents the remaining energy level in the battery, playing a crucial role in ensuring safe and efficient operation by preventing battery aging, overcharging, and deep discharge situations [11,12]. Therefore, the accurate estimation of SoC is critical to improve the performance and efficiency of electric vehicles. Many literature reviews have classified SoC estimation methods [13–15] into four parts: measured values, models, estimation algorithms, and state parameters [16–20]. Any of these SoC estimation methods use one or more estimation algorithms to estimate the state parameters in the models with the measured values and, finally, directly or indirectly estimate the SoC.

In recent years, substantial progress has been made within the field of EV battery modeling and parameter estimation to improve battery performance, lifespan, and efficiency [21,22]. The battery models utilized to determine the operation of a battery mainly fall into the following three main categories: physics-based electrochemical models [23,24], electrical equivalent circuit models (ECMs) (including the integral-order and fractional-order models) [25,26], and data-driven models established using artificial intelligence algorithms such as neural networks [27,28] and support vector machines [29]. Among these models, ECMs have gained increased interest regarding real-time applications due to their simplified model structure and easy implementation [30–32]. ECMs are used to analyze the terminal voltage output under a current profile and are typically applied in real-time situations due to their simplicity.

Parameter estimation is an important process for battery modeling systems that significantly affects the model's accuracy and reliability. In general, identification techniques can be online or offline [33,34]. In online identification techniques, model parameters can be tuned in real time according to the battery condition. The BMS employs parameters such as temperature, voltage, and current to evaluate the SoC, SoH, and SoE, which are critical for real-time monitoring. Offline identification techniques rely on experimental data and can be divided into two main categories. The first category is commonly referred to as traditional detection approaches, which include a proper technique using least squares [33], subspace estimation [34], and multiple linear regression techniques [35,36]. Despite this simple and straightforward method, estimated parameters are subject to considerable error; thus, they are generally appropriate for applications with lower accuracy standards [37,38]. The second category is known as biologically intelligent optimization algorithms, which include techniques such as particle swarm optimization (PSO) [39–42] and genetic algorithm (GA) [43,44]. This technique is regarded as more accurate and reliable, and it has become one of the most widely used approaches to identify parameters. Identifying parameters using GA comes with challenges, such as high computation times and falling into optimum local situations [42,45,46], and the PSO algorithms may exhibit low accuracy and achieve a local optimum [47,48].

In many existing articles, field data are collected over extended periods to extract and analyze the performance parameters [1,20,49,50]. For example, Pozzato et al. collected the data over a year and then analyzed the battery performance [20]. Certain studies focus on long-term battery pack data collection to evaluate battery performance [51] while others extract data based on specific conditions, such as battery signals during predefined acceleration profiles [1] or driver behavior patterns [52]. Although these approaches provide significant insights into BMS, they often rely on static or preselected conditions that may not fully reflect real-time operating scenarios. Therefore, collecting and analyzing field data under running conditions is crucial to accurately understanding how it operates in real-world scenarios.

In this work, we introduce a novel method to collect field data dynamically while the electric vehicle is in motion under real-world running conditions. Instead of relying on predefined or long-term conditions, our approach ensures that data are gathered in real time during actual vehicle operation. We then apply a novel set of conditions to this dynamic field data to ensure that sufficient and relevant data segments are selected for estimating ECM parameters. In the first step, we removed the noise from filed data and then applied first- and second-order derivatives to determine the specific data set conditions. The data set was then collected using a zero-crossing method. Finally, the ECM parameters were estimated using the PSO algorithm. The current approach provides a more realistic representation of vehicle operation and enhances the accuracy of ECM parameter estimation.

2. Fundamentals of PSO Algorithm

The PSO is a search algorithm that involves the change in the positions of particles over time [41,49]. The particles of the PSO algorithm change their position by updating their "velocity" based on their current position, which is called position best (P_{best}). Regarding its neighbor particle that is called the global best (G_{best}), the best position was found by itself and by its neighbor [50] as seen in Figure 1.

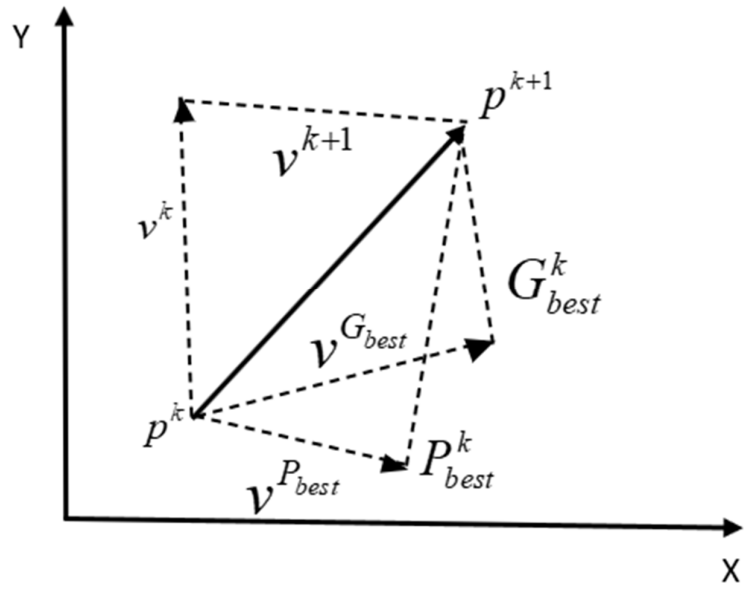


Figure 1. Fundamental concept of PSO.

The adaptation can be expressed in terms of velocity. Equation (1) can be used to update the velocity of each particle [53].

$$v^{k+1} = w.v^{k} + c_1 rand \times (P_{best} - p^{k}) + c_2 rand \times (G_{best} - p^{k}) \quad (1)$$

$$P^{k+1} = P^{k} + V^{k+1}, \quad k = 1, 2, 3, \ldots\ldots\ldots, n \quad (2)$$

Equation (1) shows how a certain velocity will gradually become closer to G_{best} and how to calculate P_{best}. Equation (2) illustrates how to update the current position. where p^{k} represents the current position of the particle, p^{k+1} shows the updated particle position, v^{k} refers to the current velocity, and v^{k+1} indicates the updated velocity. P_{best} is the best solution for the current particle, whereas G_{best} is the best solution for all particles. w represents the weight of inertia, and the rand is set to produce random numbers between 0 and 1, with c_1 and c_2 indicating positive constants.

Based on Equation (1), the PSO algorithm has three parameters, c_1 and c_2, which are acceleration coefficients, and the inertia weight (w) [54] is computed using the following Equation (3):

$$w(k) = w_{\max} - \left(\frac{w_{\max} - w_{\min}}{k_{\max}}\right) \times k \quad (3)$$

k_{max} indicates the maximum number of iterations, k refers to the current iterations, w_{max} and w_{min} represent the maximum and minimum weight of inertia, respectively. c_1 and c_2 denote the range between 1 and 2, and w_{max} and w_{min} have values of 0.9 and 0.4 [55], respectively.

The selection of these parameters plays a crucial role in determining the algorithm's performance. Fine-tuning the parameters often leads to the best performance for a specific problem. Generally, the inertia weight (w) typically decreases from 0.9 to 0.4 to transition

from a global to local search. The cognitive (c_1) and social (c_2) coefficients, usually set to 2, control individual and group learning. Swarm size (20–100 particles) and velocity limits are adjusted based on the problem, while stopping criteria like iteration limits or convergence thresholds ensure efficiency. The fine-tuning of the parameters can also be performed through trial-and-error methods. The PSO algorithm's ability to find an optimal or near-optimal solution over time is known as convergence analysis. The convergence analysis depends on the balance between exploration (high inertia, and large swarm) and exploitation (low inertia, and high cognitive/social coefficients). Careful tuning avoids premature convergence and ensures efficient search.

3. ECM for Lithium-Ion Batteries

Several battery modeling methods exist, including the ECM and electrochemical model [56–60]. The choice of the most appropriate model depends on its application, performance, and operation [59]. Some battery models are intended to perform fast real-time calculations, while others estimate the battery's state accurately [22]. ECMs simulate input and output voltage connections using circuit elements, including capacitors and resistors [57,61]. In light of the complexity of the electrochemical model, which is generally characterized by more than 20 parameters [62–64], it would be more sensible to have an ECM similar to and accurate to the electrochemical model. According to the mathematical model based on an empirical formula, the open circuit voltage (OCV) represents a polynomial function of the SoC; in model terms, it illustrates the battery's state. Moreover, it is demonstrated that the mathematical model is insufficient, with an error range of 5–20% [65]. Therefore, ECMs are one of the most widely used battery models. In the operating cycle of a battery, an ECM describes the connection between voltage and current by using a voltage source, capacitance, and resistance. The ECM consists of two circuits: the first-order resistor capacitor (FORC) circuit, and the second-order resistor capacitor (SORC) circuit.

The main parameters of the ECM, such as ohmic resistance (R_s), polarization resistance (R_p), and polarization capacitance (C_p), have distinct physical significance. R_s accounts for the resistance of the battery's internal components, such as the electrolyte, current collectors, and internal connections, and increases with temperature and battery aging. R_p shows the internal leakage current due to side reactions in the battery, and it often decreases with SoC and deteriorates with battery aging. C_p represents the ability of the battery to store charge at a given voltage and shows electrochemical behavior at the battery's electrodes. The C_p varies with SoC (increases with higher SoC), temperature, and the specific battery chemistry. Overall, these parameters detect the degradation of the battery, such as reduced capacity and efficiency under different charge/discharge conditions.

First and Second-Order RC Circuit

An electronic schematic of the FORC circuit is illustrated in Figure 2. According to Figure 2a, the V_{oc} indicates the voltage of the open circuit, Rs represents ohmic resistance, which is due to electrolytes and concentration resistance, R_{p1} and C_{p1} describe the FORC circuit model, which is polarization resistance and polarization capacitance, respectively, and V_t refers to the terminal voltage. Moreover, Kirchhoff's Voltage Law is used to determine the terminal voltage for ECM circuits, and the theoretical formula of FORC models is provided in Equation (4).

$$v_t = V_{oc} - I(R_s + R_{p1}(1 - e^{\frac{-t}{\tau}})) \tag{4}$$

$$v_t = V_{oc} - I(R_s + R_{p1}(1 - e^{\frac{-t}{\tau}}) + R_{p2}(1 - e^{\frac{-t}{\tau}})) \tag{5}$$

where $\tau = R_{p1} \times C_{p1}$.

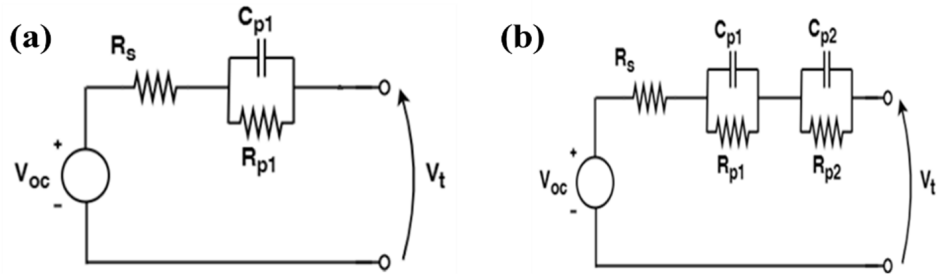


Figure 2. (**a**) ECM with FORC and (**b**) ECM with FORC and SORC.

The combined electronic schematic diagram of the ECM is shown in Figure 2b. It can be observed that V_{oc}, R_s, R_{p1}, C_{p1}, and Vt are the same as those in FORC; however, in the SORC, R_{p2}, and C_{p2} refer to non-linear polarization resistance and capacitance, respectively. Additionally, Kirchhoff's Voltage Law is applied to determine the terminal voltage in ECM circuits, and the mathematical formula for SORC models is given in Equation (5).

A comparison of the output from the FORC and SORC models can be seen in Figure 3. It appears that the combined electronic model (FORC + SORC) is consistent with the real voltage. Furthermore, it is worth noting that the SORC for ECM has been widely adopted and is more accurate and performs better than FORC.

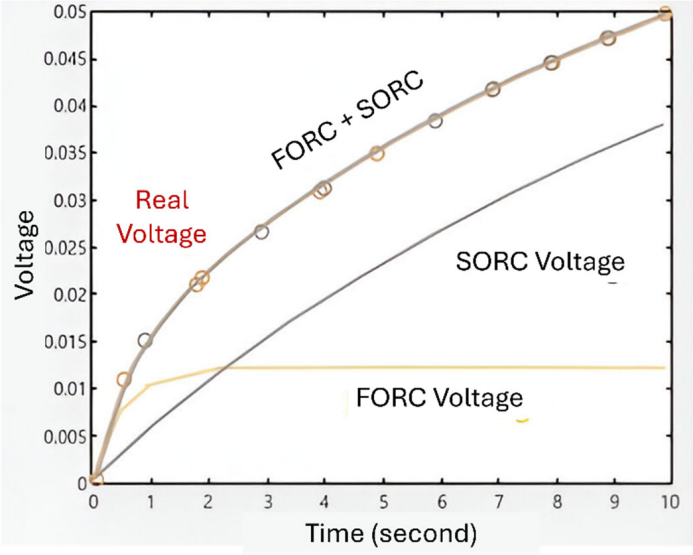


Figure 3. Comparison of the output from the FORC and SORC models.

4. Proposed Methodology for Collecting Data

4.1. Experimental Data

A Battery Tester (BT) manufactured by FAMTECH was employed for the experiment, as presented in Figure 4. The Li-ion battery with a capacity of 2.1 Ah was charged and discharged several times and controlled by a PC using the software NEWARE BTS 7.6.0. The voltage was in the range of 0–10 V, and the current was in the range of 0–8 A. The battery was charged and discharged 3 times via the Constant Current Constant Voltage Charge (CCCV-Chrg) and Constant Current Constant Voltage DisCharge (CCCV-DChg) command to activate the new battery. After the activation, the battery was charged at a 0.5 C rate for 12 min and then held for 10 min to find the ECM parameters. This process is repeated until the voltage reaches 4.2 volts. In this step, the battery is discharged at a 0.5 C rate for 12 min and then maintained for 10 min rest; the process is repeated until the voltage reaches 2.5 V. According to the battery's capacity and C rate, the battery is charged

and discharged in 12 min for a 10% SoC difference. In Table 1, we describe the experimental procedure in detail.

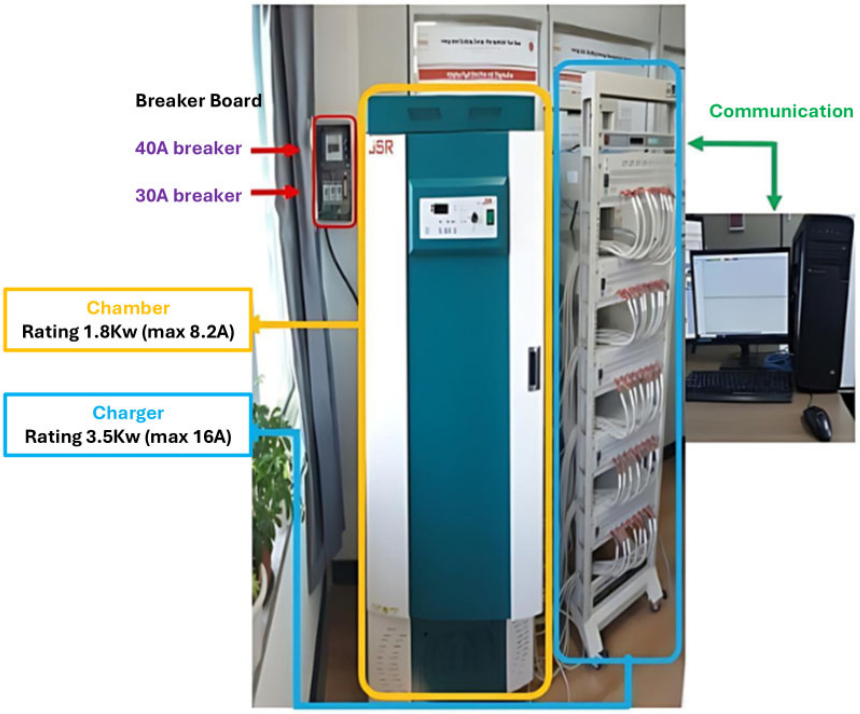


Figure 4. Battery tester setup (BT).

Table 1. Experimental procedure.

ID	Status	Time (hh:mm:ss:ms)	Cycle	Voltage (V)	Current (A)
1	CCCV_Chg			4.200	1.05
2	Rest	00:10:00:00			
3	CCCV_DChg			2.500	1.05
4	Rest	00:10:00:00			
5	Cycle	Begin ID: 1	Times: 3		
6	CC_Chg	00:12:00:00		4.200	1.05
7	Rest	00:10:00:00			
8	Cycle	Begin ID: 6	Times: 10		
9	CC_Dchg	00:12:00:00		2.500	1.05
10	Rest	00:10:00:00			
11	Cycle	Begin ID: 9	Times: 10		

Using Matlab, the experimental data were retrieved from NEWARE BTS software and converted into standard form (T, V, I, and *SoC*), where T, V, and I represent the time, voltage, and current, respectively. The *SoC* of the experimental data is obtained using Equation (6).

$$SoC(\%) = \frac{Battery_Cap - Discharge_Cap}{Battery_Cap} \times 100 \quad (6)$$

4.2. Proposed Methodology for Retrieving Field Data

Following the experimental data collection and verification of the results, we developed a method to retrieve and determine the parameters of field data for electric vehicles

(running conditions). Figure 5a demonstrates a part of the field data that was extremely challenging to analyze. In the first step of analyzing the field data (Figure 5a), we removed the spikes in voltage by using Matlab's moving_avg function, as shown in Figure 5b. We employed the function to implement single-dimensional filtering. During the filtering process, a window of length (size of the window) is slid along with the data, and the average of the data contained in the window is calculated. Figure 5b illustrates that moving_avg determines the mean value of the data based on the window size. The plot in Figure 5c shows the result of the moving_avg, representing the average of the field data with reduced noise. Further, Figure 6 displays the Matlab code for the moving_avg filter function.

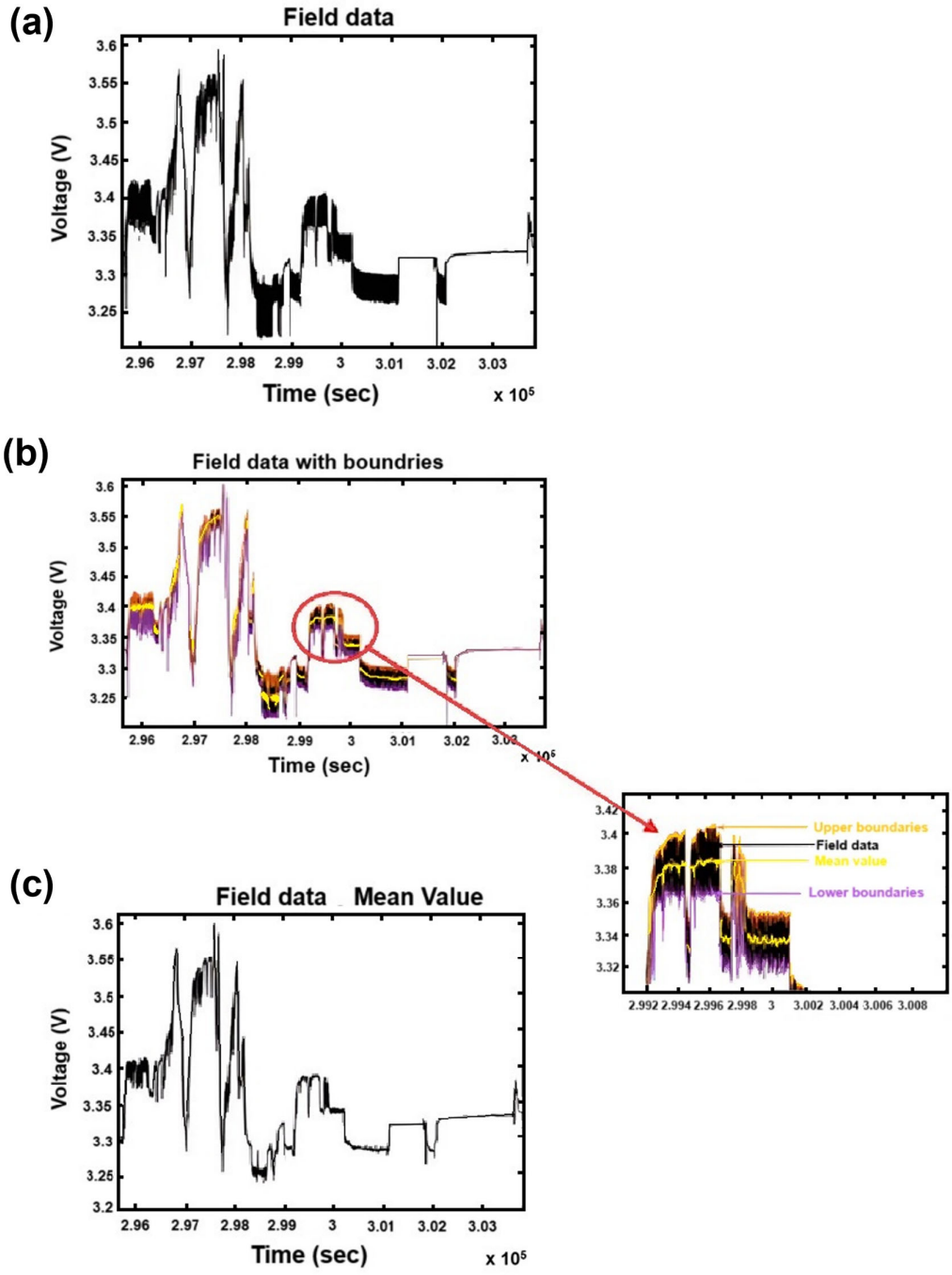


Figure 5. (**a**) Field data; (**b**) field data with moving_avg function; (**c**) field data after noise is removed.

```
function out = Movingavg(in,N)
if(isempty(in))||(n<=0)
fprintf('Movi ng_avg(error) empty input data or n null.\n');
return;
end
if(N==1)
out = in;
return;
end
nx = length(in);
if (N>=(2*(nx-1)))
out = mean(in)*ones(size(in));
return;
end
out = zeros(size(in));
if rem(N,2)~=1
m= N/2;
else
m= (N-1/2);
end
for i = 1:nx
dist2start = i-1;
dist2end = nx-1;
if dist2start < N|| dist2end<N
dd = min (dist2start, dist2end);
else
dd = m;
end
out(i) = mean (in(i-dd:i+dd));
end
end
```

Figure 6. Matlab code for the function of moving average filter.

The derivative of the current for time, which is selected from the field data to detect zero-crossing points, is shown in Figure 7a. These zero-crossings are essential for extracting specific parts of the field data for further examination. We selected portions of the field data under specified conditions based on these zero-crossing points. Figure 7b shows the voltage data, with the points where the value crosses zero marked by the matching points in the current's derivative. We further improved the selection process by considering the data segments with more than 100 points. This condition is important because smaller data sets can lead to inaccuracies in parameter estimation. By implementing this approach, the selection of field data is optimized to secure reliable and consistent results. Figure 7c shows the selected part of the field data using the zero-crossing method. The selected segment of the field data, retrieved through the zero-crossing method, is shown in Figure 8a. This segment highlights the portion of data identified based on predefined selection criteria. For estimating the ECM parameters, we use real retrieved field data and retrieved field data after filtering.

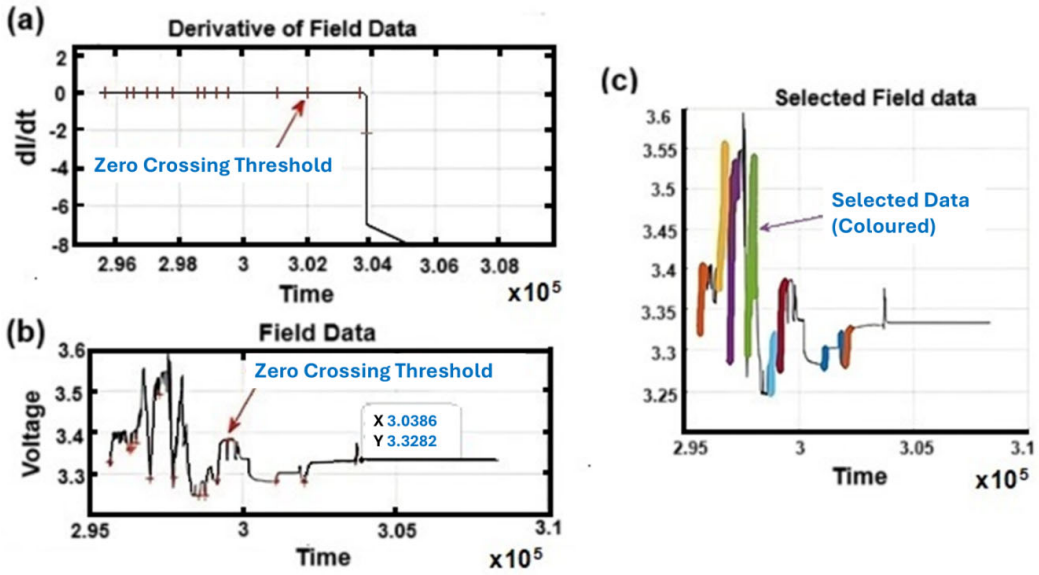


Figure 7. (**a**) shows the derivative of the current with respect to time, (**b**) represents the voltage field data as a function of time, with the red dots indicating the zero-crossing points, and (**c**) shows that the colored part is the selected field data.

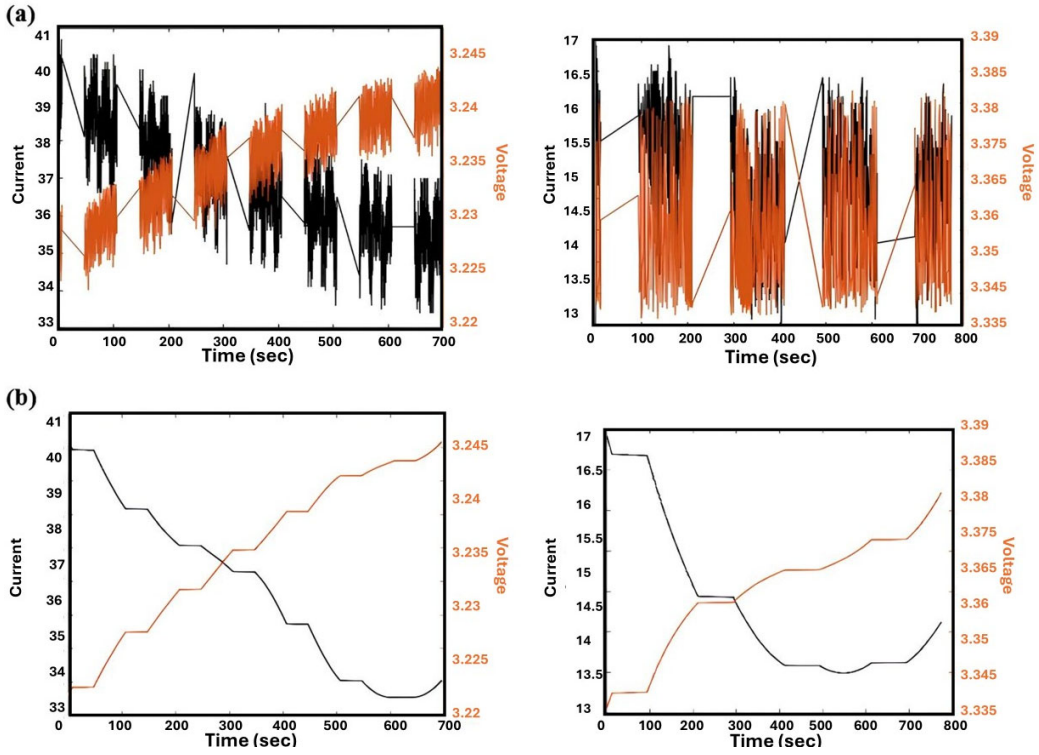


Figure 8. (**a**) Retrieved field data; (**b**) retrieved field data after filtering.

Figure 9 illustrates the flowchart of the proposed methodology, retrieving field data and the algorithm used to estimate the ECM parameters. Field data contain noise, which is challenging to analyze; we offer a method to make the data smooth to analyze quickly; first, we applied a moving average filter, as shown in Figure 5c, to remove the noise from the data. After filtering the data, we applied common conditions for retrieving field data. Firstly, we applied a first- and second-order derivative to produce the data between the positive and negative axes. Then, we used a zero-crossing method [66], as shown in Figure 7a, to find when the data crosses zero, it starts achieving the data, and when another zero-crossing

occurs, it stops obtaining the data. Using this method, we retrieved some parts of the field data. We estimated ECM parameters using PSO for both the filtered data and real selected data, as shown in Figure 8a,b.

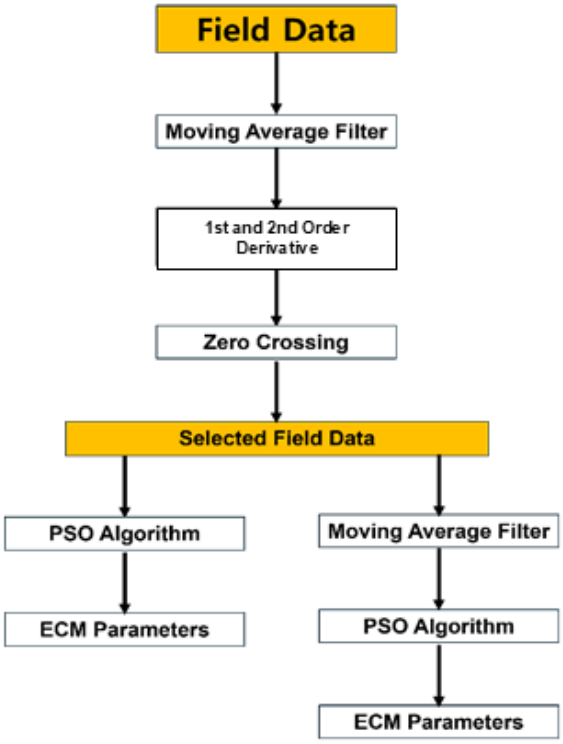


Figure 9. Methodology for retrieving field data and estimating ECM parameters.

5. Results and Validation

5.1. Simulation

After interpreting the experimental data retrieved in Section 4, it was converted into standard form (V, I, t, and SoC) and divided into charge pulse, discharge pulse, and rest data to obtain the ECM parameters with the PSO algorithm. The objective function of the PSO algorithm is presented below in Formula (7) [67,68].

$$\overline{V} = I \times (R_{p1}(1 - e^{\frac{-t}{\tau}}) + R_{p2}(1 - e^{\frac{-t}{\tau}})) \tag{7}$$

where $\tau = R_p \times C_p$, and $\overline{V}$ indicates the measured ECM voltage.

The flow chart of the PSO algorithm is shown in Figure 10. The parameters used in the PSO algorithm can be found in Table 2. The PSO parameters in this study were chosen based on a trial-and-error approach to achieve a balance between exploration (global search) and exploitation (local search), as recommended in established PSO literature [41,49,50]. The cognitive and social coefficients were carefully selected to ensure equal influence of both the personal best and global best positions and facilitate effective convergence to the optimal solution. For simplicity and computational efficiency, fixed coefficients were employed, as they have been shown to provide reliable performance in parameter estimation problems. Furthermore, multiple independent runs of the PSO algorithm were conducted to verify the robustness of the results. A robust stopping criterion, based on the stabilization of fitness values and the maximum allowable number of iterations, was applied to ensure convergence and to mitigate the risk of premature termination. For parameters identification, we need voltage over potential (V_{op}) data; thus, the data we

retrieved from BT also contains rest data and open circuit voltage (OCV). Open circuit voltage (OCV) is omitted from real data to obtain accurate parameters; hence, the OCV part is removed by using a straight-line equation (y = m.x + C) [69] as shown in Equations (8) and (9), which are plotted in Figure 11.

$$OCV = m \times t \tag{8}$$

$$m = \frac{y_2 - y_1}{x_2 - x_1} \tag{9}$$

where y = Voltage, x = time.

$$v_{op} = v_r - OCV \tag{10}$$

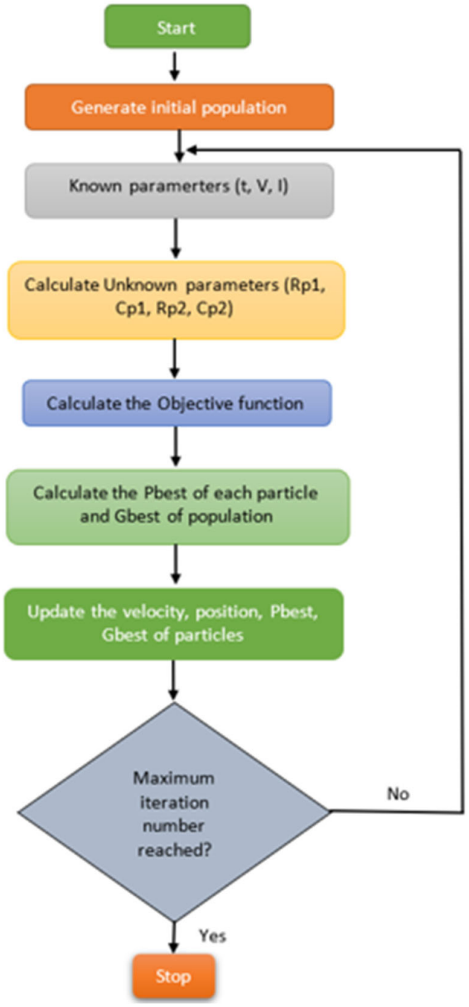


Figure 10. PSO flow chart.

Table 2. Parameters for PSO algorithm.

Parameters	Value
w	0.690
c_1	1.623
c_2	1.623
No. of Particles	50
Maximum No. of Iteration	250

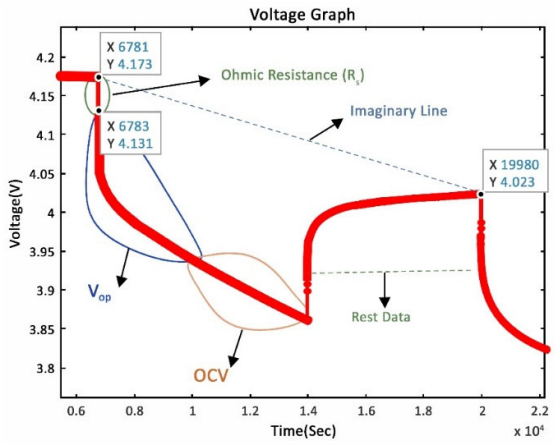


Figure 11. Voltage with OCV impact.

Here, V_{op} denotes an overpotential voltage, and v_r represents the real voltage derived from experimental data, as discussed in Section 4. The data retrieved from BT are divided into charge and discharge pulses from which the OCV part is removed, and the V_{op} part is shown in Figure 12a,b. The ECM parameters are estimated for the v_{op} part of the retrieved data.

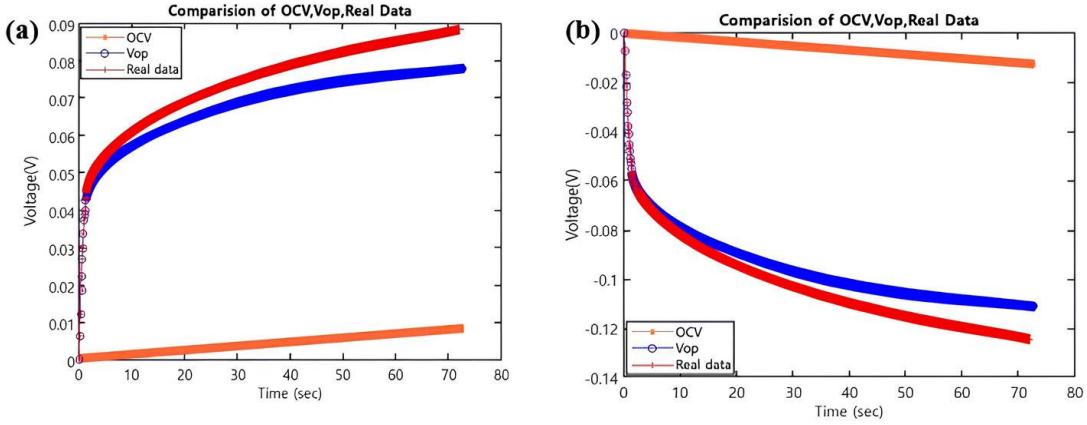


Figure 12. (**a**) Charge pulse; (**b**) discharge pulse.

Figure 13a compares the charge pulse parameters, real data, and voltage gap, and (b) compares discharge pulse parameters, real data, and voltage gap. The OCV is the estimated value obtained using the line equation. The difference between OCV and real data is known as the voltage gap. By comparing the voltage gap, which is the v_{op} part of the real data, with simulated data obtained by using the ECM parameters, we find that the simulated data follows the pattern of the v_{op} part accurately, and the RMSE is considerably less than 2%. This error is considered a random error, arising due to the inherent noise in the data, and was introduced during the filtering process and the application of the zero-crossing method for data retrieval. Additionally, the PSO algorithm used for parameter estimation inherently introduces approximation-based error due to the stochastic nature of the optimization process. This error might be further reduced by improving the filtering method, which can remove the noise from the data without affecting the real data, or by improving the optimization algorithm using a hybrid algorithm. Furthermore, we have recognized from previous studies that including additional factors, such as temperature and battery aging, in the modeling process can enhance the reliability and applicability of the proposed method. These factors will allow for a more accurate representation of real-world operating conditions and provide a more environmentally adaptive framework.

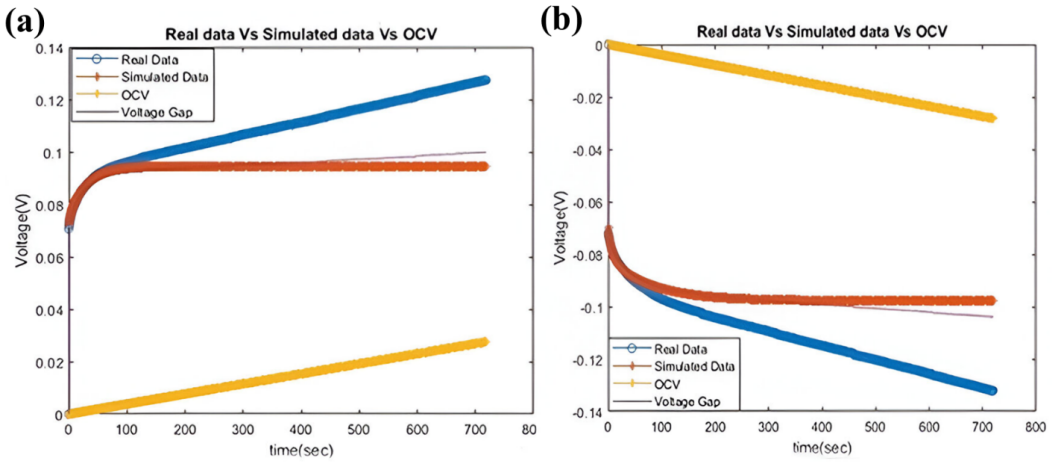


Figure 13. (**a**) Comparison of real data and simulation data without OCV impact for charge pulse. (**b**) Comparison of real data and simulation data without OCV impact for discharge pulse.

5.2. Results for Field Data

Figure 14a illustrates the comparison between real data and terminal voltage (V_t), which is simulated data. The terminal voltage follows the pattern of real data, showing that the ECM parameters estimated by PSO are accurate. The ECM parameters estimated for filtered data are compared with filtered real data are shown in Figure 14b. To find the terminal voltage (V_t), we use the ECM Formula (11).

$$V_t = OCV - I \times (Rs + R_{p1}(1 - e^{\frac{-t}{\tau}}) + R_{p2}(1 - e^{\frac{-t}{\tau}})) \tag{11}$$

where $\tau = R_p \times C_p$, OCV is the open circuit voltage, and R_s is the ohmic resistance.

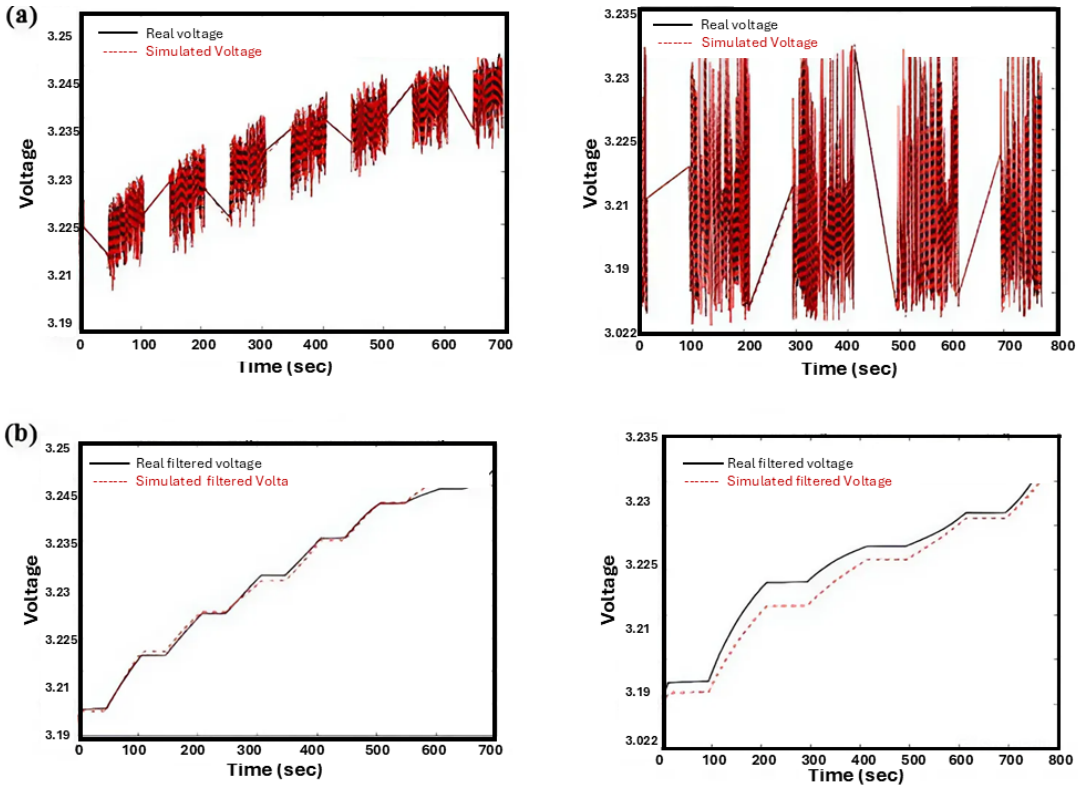


Figure 14. (**a**) Comparison of real voltage and terminal voltage. (**b**) Comparison of filtered real voltage and filtered terminal voltage.

6. Discussion

In this study, we collected the field data in real-time while the vehicle was in motion. This ensures that the data reflects actual operating conditions. Furthermore, we apply specific criteria to the retrieved data to ensure it is sufficient and relevant for estimating ECM parameters, overcoming the limitations of static data collection approaches. In many studies, field data are collected under specific or static conditions. For example, some researchers collect battery pack data over extended periods, such as one year, to evaluate performance [20]. Others focus on specific scenarios, such as acceleration profiles [1] or driver behavior [52]. While these approaches provide valuable insights, they often fail to capture the dynamic and real-time nature of EV operation. The novelty of our work lies in the collection of field data in real-time while the vehicle is in motion. This ensures that the data reflects actual operating conditions. For parameter estimation, we employed PSO [41] because it is highly efficient in handling complex, multidimensional optimization problems and is less computationally intensive compared to algorithms like Genetic Algorithm (GA) or Grey Wolf Optimizer (GWO) [70]. Unlike the least squares method and Kalman Filter, PSO does not require gradient information, thus making it robust against non-linearities in the data. Additionally, PSO is simpler to implement than the hybrid optimization techniques and does not suffer from issues like premature convergence, which are common in GA.

The use of the ECM [56,58] offers significant advantages due to its simplicity, adaptability, and computational efficiency. It is particularly suited for real-time BMS, providing a good balance between accuracy and practicality. In contrast, Electrochemical Models, while more precise, require high computational resources and detailed modeling efforts, making them less feasible for real-time use. Data-driven models, on the other hand, lack interpretability and rely heavily on extensive datasets, which may not always be available or accurate [16].

The proposed method has significant potential for the accurate and reliable parameter estimation of ECMs. Particularly, it is valuable for real-time battery management systems BMS in EVs, where accurate estimation of battery states, such as SoC and SoH, are critical for ensuring safety, optimizing performance, and extending battery life. Furthermore, the PSO algorithm enhances the precision of ECMs, even under running battery conditions. This makes the method applicable not only to conventional EV batteries but also to other advanced energy storage systems, such as hybrid electric vehicles and stationary energy storage units. Additionally, the flexibility of the proposed approach allows it to adapt to various battery systems and charging/discharging strategies, which will further expand its practical utility. A key strength of our work lies in the validation of the retrieved and estimated parameters through comprehensive curve fitting against real-world field data. This demonstrates the theoretical performance and practical applicability of the proposed. By addressing key challenges in battery modeling, this study provides a foundation for improving the efficiency and reliability of next-generation energy management systems.

Despite the promising outcomes, the proposed data retrieval method has some sensitive factors and limitations. Primarily, the noise filtering process, zero-crossing threshold, data selection conditions, and the parameters of the PSO algorithm are sensitive factors for this study. These factors require careful tuning and consideration, as improper settings can significantly degrade performance and lead to inaccurate results. For example, the noise removal process depends on the window size of the moving-average filter; a larger window size makes data oversmooth, and a smaller window may fail to reduce noise. Similarly, the improper zero-crossing threshold selection can lead to either missed crossings or the inclusion of irrelevant ones. The data selection conditions are also critical because the minimum number of points or time intervals may exclude useful data, while lenient conditions

might allow noisy or irrelevant data to affect parameter estimation. Additionally, as we discussed earlier, the PSO algorithm used for parameter estimation inherently introduces approximation-based error, which is the main limitation of this method. In our work, this error is around 2% which might be further reduced by improving the optimization algorithm using a hybrid algorithm method or including additional factors, such as temperature and battery aging. Future work aims to address these issues to allow for a more accurate representation of real-world operating conditions and provide a more environmentally adaptive framework.

7. Conclusions

This paper proposes an efficient method to estimate the ECM parameters (Rp and Cp) from the field data (voltage, current, and time). Firstly, the noise from field data was removed using a moving average filter. After that first- and second-order derivations are applied to the filtered data to determine a specific data set of conditions and then introduce a novel zero-crossing technique for retrieving meaningful data segments. The selected field data were then analyzed using a second-order RC model. Finally, a PSO algorithm has been adapted to estimate the parameters of the SORC. It was concluded that the error between simulation and real voltage is less than 2% (calculated above 100 points), which signifies that the PSO is a better parameter identification approach than others. However, this error can be further reduced by improving the filtering method and optimization algorithm by using the hybrid algorithm. Furthermore, including temperature and battery aging in the modeling process can enhance the reliability and applicability of the proposed method. Looking ahead, we plan to focus on the hybrid approach and incorporate temperature and battery aging factors into our model to further enhance its accuracy. These additions will allow the ECM parameters to accurately estimate the state of the battery for long-term battery performance and environmental influences, making it more applicable for real-world applications.

Author Contributions: Conceptualization, S.A.S.; methodology, S.A.S.; software, S.A.S. and S.I.; validation, S.I. and J.P.; formal analysis, S.A.S. and S.H.; investigation, S.H. and W.Y.K.; resources, S.H. and J.P.; data curation, S.A.S. and S.H.; writing—original draft preparation, S.A.S. and J.P.; writing—review and editing, S.I., S.H. and W.Y.K.; visualization, S.A.S.; supervision, S.H. and W.Y.K.; project administration, S.H. and W.Y.K.; funding acquisition, W.Y.K. All authors have read and agreed to the published version of the manuscript.

Funding: This research was supported by the "Regional Innovation Strategy (RIS)" through the National Research Foundation of Korea (NRF), funded by the Ministry of Education (MOE) (2023-RIS009).

Institutional Review Board Statement: Not applicable.

Informed Consent Statement: Not applicable.

Data Availability Statement: Data are contained within the article.

Conflicts of Interest: The authors declare that they have no known competing financial interests or personal relationships that could have appeared to influence the work reported in this paper.

References

1. Barr, A.; Suard, F.; Gérard, M.; Riu, D. A Real-time Data-driven Method for Battery Health Prognostics in Electric Vehicle Use. *PHM Soc. Eur. Conf.* **2014**, *2*, 1–8. [CrossRef]
2. Patil, P. Innovations in electric vehicle technology: A review of emerging trends and their potential impacts on transportation and society. *Rev. Contemp. Bus. Anal.* **2021**, *4*, 1–13.
3. Dik, A.; Omer, S.; Boukhanouf, R. Electric Vehicles: V2G for Rapid, Safe, and Green EV Penetration. *Energies* **2022**, *15*, 803. [CrossRef]

4. See, K.; Wang, G.; Zhang, Y.; Wang, Y.; Meng, L.; Gu, X.; Zhang, N.; Lim, K.; Zhao, L.; Xie, B. Critical review and functional safety of a battery management system for large-scale lithium-ion battery pack technologies. *Int. J. Coal Sci. Technol.* **2022**, *9*, 36. [CrossRef]
5. Gabbar, H.A.; Othman, A.M.; Abdussami, M.R. Review of Battery Management Systems (BMS) Development and Industrial Standards. *Technologies* **2021**, *9*, 28. [CrossRef]
6. Hu, X.; Feng, F.; Liu, K.; Zhang, L.; Xie, J.; Liu, B. State estimation for advanced battery management: Key challenges and future trends. *Renew. Sustain. Energy Rev.* **2019**, *114*, 109334. [CrossRef]
7. Ungurean, L.; Cârstoiu, G.; Micea, M.V.; Groza, V. Battery state of health estimation: A structured review of models, methods and commercial devices. *Int. J. Energy Res.* **2017**, *41*, 151–181. [CrossRef]
8. Li, Y.; Stroe, D.-I.; Cheng, Y.; Sheng, H.; Sui, X.; Teodorescu, R. On the feature selection for battery state of health estimation based on charging–discharging profiles. *J. Energy Storage* **2021**, *33*, 102122. [CrossRef]
9. Shen, P.; Ouyang, M.; Lu, L.; Li, J.; Feng, X. The co-estimation of state of charge, state of health, and state of function for lithium-ion batteries in electric vehicles. *IEEE Trans. Veh. Technol.* **2017**, *67*, 92–103. [CrossRef]
10. Ma, L.; Hu, C.; Cheng, F. State of charge and state of energy estimation for lithium-ion batteries based on a long short-term memory neural network. *J. Energy Storage* **2021**, *37*, 102440. [CrossRef]
11. Ouyang, D.; Weng, J.; Chen, M.; Wang, J.; Wang, Z. Sensitivities of lithium-ion batteries with different capacities to overcharge/over-discharge. *J. Energy Storage* **2022**, *52*, 104997. [CrossRef]
12. Chen, S.; Fan, G.; Wang, Y.; Zhou, B.; Ye, S.; Liu, Y.; Guo, B.; Zhu, C.; Zhang, X. The impact of intermittent overcharging on battery capacity and reliability: Electrochemical performance analysis and failure prediction. *J. Power Sources* **2024**, *591*, 233800. [CrossRef]
13. Xiong, R.; Cao, J.; Yu, Q.; He, H.; Sun, F. Critical Review on the Battery State of Charge Estimation Methods for Electric Vehicles. *IEEE Access* **2018**, *6*, 1832–1843. [CrossRef]
14. Zheng, Y.; Ouyang, M.; Han, X.; Lu, L.; Li, J. Investigating the error sources of the online state of charge estimation methods for lithium-ion batteries in electric vehicles. *J. Power Sources* **2018**, *377*, 161–188. [CrossRef]
15. Adaikkappan, M.; Sathiyamoorthy, N. Modeling, state of charge estimation, and charging of lithium-ion battery in electric vehicle: A review. *Int. J. Energy Res.* **2022**, *46*, 2141–2165. [CrossRef]
16. How, D.N.; Hannan, M.; Lipu, M.H.; Ker, P.J. State of charge estimation for lithium-ion batteries using model-based and data-driven methods: A review. *IEEE Access* **2019**, *7*, 136116–136136. [CrossRef]
17. Shrivastava, P.; Soon, T.K.; Idris, M.Y.I.B.; Mekhilef, S. Overview of model-based online state-of-charge estimation using Kalman filter family for lithium-ion batteries. *Renew. Sustain. Energy Rev.* **2019**, *113*, 109233. [CrossRef]
18. Li, B.; Bei, S. Estimation algorithm research for lithium battery SOC in electric vehicles based on adaptive unscented Kalman filter. *Neural Comput. Appl.* **2019**, *31*, 8171–8183. [CrossRef]
19. Naseri, F.; Schaltz, E.; Stroe, D.-I.; Gismero, A.; Farjah, E. An enhanced equivalent circuit model with real-time parameter identification for battery state-of-charge estimation. *IEEE Trans. Ind. Electron.* **2021**, *69*, 3743–3751. [CrossRef]
20. Pozzato, G.; Allam, A.; Pulvirenti, L.; Negoita, G.A.; Paxton, W.A.; Onori, S. Analysis and key findings from real-world electric vehicle field data. *Joule* **2023**, *7*, 2035–2053. [CrossRef]
21. Nachimuthu, S.; Alsaif, F.; Devarajan, G.; Vairavasundaram, I. Real time SOC estimation for Li-ion batteries in Electric vehicles using UKBF with online parameter identification. *Sci. Rep.* **2025**, *15*, 1714. [CrossRef] [PubMed]
22. Wang, Y.; Tian, J.; Sun, Z.; Wang, L.; Xu, R.; Li, M.; Chen, Z. A comprehensive review of battery modeling and state estimation approaches for advanced battery management systems. *Renew. Sustain. Energy Rev.* **2020**, *131*, 110015. [CrossRef]
23. Tian, A.; Dong, K.; Yang, X.-G.; Wang, Y.; He, L.; Gao, Y.; Jiang, J. Physics-based parameter identification of an electrochemical model for lithium-ion batteries with two-population optimization method. *Appl. Energy* **2025**, *378*, 124748. [CrossRef]
24. Yavuz, H.; Akyildiz, A.; Gulbahce, M.O. A Comprehensive Review of Physics-Based Battery Models and Comparing Different Physics-Based Models for Various Chemistries. *Turk. J. Electr. Power Energy Syst.* **2024**, *4*, 108–117. [CrossRef]
25. Su, J.; Lin, M.; Wang, S.; Li, J.; Coffie-Ken, J.; Xie, F. An equivalent circuit model analysis for the lithium-ion battery pack in pure electric vehicles. *Meas. Control* **2019**, *52*, 193–201. [CrossRef]
26. Tran, M.-K.; Mathew, M.; Janhunen, S.; Panchal, S.; Raahemifar, K.; Fraser, R.; Fowler, M. A comprehensive equivalent circuit model for lithium-ion batteries, incorporating the effects of state of health, state of charge, and temperature on model parameters. *J. Energy Storage* **2021**, *43*, 103252. [CrossRef]
27. Kara, A. A data-driven approach based on deep neural networks for lithium-ion battery prognostics. *Neural Comput. Appl.* **2021**, *33*, 13525–13538. [CrossRef]
28. Li, W.; Demir, I.; Cao, D.; Jöst, D.; Ringbeck, F.; Junker, M.; Sauer, D.U. Data-driven systematic parameter identification of an electrochemical model for lithium-ion batteries with artificial intelligence. *Energy Storage Mater.* **2022**, *44*, 557–570. [CrossRef]
29. Xuan, L.; Qian, L.; Chen, J.; Bai, X.; Wu, B. State-of-charge prediction of battery management system based on principal component analysis and improved support vector machine for regression. *IEEE Access* **2020**, *8*, 164693–164704. [CrossRef]

30. Bhushan, N.; Mekhilef, S.; Tey, K.S.; Shaaban, M.; Seyedmahmoudian, M.; Stojcevski, A. Overview of model-and non-model-based online battery management systems for electric vehicle applications: A comprehensive review of experimental and simulation studies. *Sustainability* **2022**, *14*, 15912. [CrossRef]
31. Hussein, H.M.; Aghmadi, A.; Abdelrahman, M.S.; Rafin, S.S.H.; Mohammed, O. A review of battery state of charge estimation and management systems: Models and future prospective. *Wiley Interdiscip. Rev. Energy Environ.* **2024**, *13*, e507.
32. Gao, Y.; Zhu, C.; Zhang, X.; Guo, B. Implementation and evaluation of a practical electrochemical-thermal model of lithium-ion batteries for EV battery management system. *Energy* **2021**, *221*, 119688. [CrossRef]
33. Ren, B.; Xie, C.; Sun, X.; Zhang, Q.; Yan, D. Parameter identification of a lithium-ion battery based on the improved recursive least square algorithm. *IET Power Electron.* **2020**, *13*, 2531–2537. [CrossRef]
34. Camboim, M.M.; Moreira, A.C.; Giesbrecht, M. Parameter Estimation of Second-Life Lithium-Ion Batteries Through Subspace Identification Methods. In Proceedings of the 2023 IEEE 32nd International Symposium on Industrial Electronics (ISIE), Helsinki, Finland, 19–21 June 2023; pp. 1–6.
35. Zhu, H.; Liu, Y.; Zhao, C. Parameter identification and SOC estimation of lithium ion battery. *Hunan Daxue Xuebao/J. Hunan Univ. Nat. Sci.* **2014**, *41*, 37–42.
36. Hong, J.; Wang, Z.; Chen, W.; Wang, L.-Y.; Qu, C. Online joint-prediction of multi-forward-step battery SOC using LSTM neural networks and multiple linear regression for real-world electric vehicles. *J. Energy Storage* **2020**, *30*, 101459. [CrossRef]
37. Tamilselvi, S.; Gunasundari, S.; Karuppiah, N.; Razak RK, A.; Madhusudan, S.; Nagarajan, V.M.; Sathish, T.; Shamim, M.Z.M.; Saleel, C.A.; Afzal, A. A review on battery modelling techniques. *Sustainability* **2021**, *13*, 10042. [CrossRef]
38. Feng, F.; Hu, X.; Hu, L.; Hu, F.; Li, Y.; Zhang, L. Propagation mechanisms and diagnosis of parameter inconsistency within Li-Ion battery packs. *Renew. Sustain. Energy Rev.* **2019**, *112*, 102–113. [CrossRef]
39. Kennedy, J.; Eberhart, R. Particle swarm optimization. In Proceedings of the ICNN'95-International Conference on Neural Networks, Perth, WA, Australia, 27 November–1 December 1995; pp. 1942–1948.
40. Usama, M.; Kim, J. Model-free current control solution employing intelligent control for enhanced motor drive performance. *Sci. Rep.* **2025**, *15*, 60. [CrossRef]
41. Wang, D.; Tan, D.; Liu, L. Particle swarm optimization algorithm: An overview. *Soft Comput.* **2018**, *22*, 387–408. [CrossRef]
42. Jusoh, M.A.; Daud, M.Z. Accurate battery model parameter identification using heuristic optimization. *Int. J. Power Electron. Drive Syst.* **2020**, *11*, 333. [CrossRef]
43. Lambora, A.; Gupta, K.; Chopra, K. Genetic algorithm-A literature review. In Proceedings of the 2019 International Conference on Machine Learning, Big Data, Cloud and Parallel Computing (COMITCon), Faridabad, India, 14–16 February 2019; pp. 380–384.
44. Fatima Brondani, M.d.; Sausen, A.T.Z.R.; Sausen, P.S.; Binelo, M.O. Parameter estimation of lithium ion polymer battery mathematical model using genetic algorithm. *Comput. Appl. Math.* **2018**, *37*, 296–313. [CrossRef]
45. Ou, C.; Lin, W. Comparison between PSO and GA for parameters optimization of PID controller. In Proceedings of the 2006 International Conference on Mechatronics and Automation, Luoyang, China, 15–18 June 2006; pp. 2471–2475.
46. Kachitvichyanukul, V. Comparison of three evolutionary algorithms: GA, PSO, and DE. *Ind. Eng. Manag. Syst.* **2012**, *11*, 215–223. [CrossRef]
47. Zhang, Y.; Wang, S.; Ji, G. A comprehensive survey on particle swarm optimization algorithm and its applications. *Math. Probl. Eng.* **2015**, *2015*, 931256. [CrossRef]
48. Noel, M.M. A new gradient based particle swarm optimization algorithm for accurate computation of global minimum. *Appl. Soft Comput.* **2012**, *12*, 353–359. [CrossRef]
49. Eberhart, R.; Kennedy, J. A new optimizer using particle swarm theory. In Proceedings of the MHS'95 Sixth International Symposium on Micro Machine and Human Science, Nagoya, Japan, 4–6 October 1995; pp. 39–43.
50. Wen, C.; Ling, W.; Ren, X. General particle swarm optimization algorithm. In Proceedings of the 2023 IEEE 2nd International Conference on Electrical Engineering, Big Data and Algorithms (EEBDA), Changchun, China, 24–26 February 2023; pp. 1204–1208.
51. Song, L.; Zhang, K.; Liang, T.; Han, X.; Zhang, Y. Intelligent state of health estimation for lithium-ion battery pack based on big data analysis. *J. Energy Storage* **2020**, *32*, 101836. [CrossRef]
52. D Pranav, O.; Babu, P.S.; Indragandhi, V.; Ashok, B.; Vedhanayaki, S.; Kavitha, C. Enhanced SOC estimation of lithium ion batteries with RealTime data using machine learning algorithms. *Sci. Rep.* **2024**, *14*, 16036. [CrossRef]
53. Jaberipour, M.; Khorram, E.; Karimi, B. Particle swarm algorithm for solving systems of nonlinear equations. *Comput. Math. Appl.* **2011**, *62*, 566–576. [CrossRef]
54. Wang, S.; Zhou, F.; Wang, F. Effect of Inertia Weight w on PSO-SA Algorithm. *Int. J. Online Biomed. Eng. (Ijoe)* **2013**, *9*, 87–91. [CrossRef]
55. Eberhart, R.C.; Shi, Y. Comparing inertia weights and constriction factors in particle swarm optimization. In Proceedings of the 2000 Congress on Evolutionary Computation. CEC00 (Cat. No. 00TH8512), La Jolla, CA, USA, 16–19 July 2000; pp. 84–88.
56. Thakkar, R.R.; Rao, Y.S.; Sawant, R.R. Performance Analysis of Electrical Equivalent Circuit Models of Lithium-ion Battery. In Proceedings of the 2020 IEEE Pune Section International Conference (PuneCon), Pune, India, 16–18 December 2020; pp. 103–107.

57. Rushali, R.T. Electrical Equivalent Circuit Models of Lithium-ion Battery. In *Management and Applications of Energy Storage Devices*; Kenneth, E.O., Ed.; IntechOpen: Rijeka, Croatia, 2021; Chapter 1. [CrossRef]
58. Rukavina, F.; Leko, D.; Matijašić, M.; Bralić, I.; Ugalde, J.M.; Vašak, M. Identification of Equivalent Circuit Model Parameters for a Li-ion Battery Cell. In Proceedings of the 2023 IEEE 11th International Conference on Systems and Control (ICSC), Sousse, Tunisia, 18–20 December 2023; pp. 671–676.
59. Tran, M.-K.; DaCosta, A.; Mevawalla, A.; Panchal, S.; Fowler, M. Comparative Study of Equivalent Circuit Models Performance in Four Common Lithium-Ion Batteries: LFP, NMC, LMO, NCA. *Batteries* **2021**, *7*, 51. [CrossRef]
60. Santos, R.M.S.; Alves, C.L.G.d.S.; Macedo, E.C.T.; Villanueva, J.M.M.; Hartmann, L.V. Estimation of lithium-ion battery model parameters using experimental data. In Proceedings of the 2017 2nd International Symposium on Instrumentation Systems, Circuits and Transducers (INSCIT), Fortaleza, Brazil, 28 August–1 September 2017; pp. 1–6.
61. Yang, J.; Cai, Y.; Pan, C.; Mi, C. A novel resistor-inductor network-based equivalent circuit model of lithium-ion batteries under constant-voltage charging condition. *Appl. Energy* **2019**, *254*, 113726. [CrossRef]
62. Li, W.; Cao, D.; Jöst, D.; Ringbeck, F.; Kuipers, M.; Frie, F.; Sauer, D.U. Parameter sensitivity analysis of electrochemical model-based battery management systems for lithium-ion batteries. *Appl. Energy* **2020**, *269*, 115104. [CrossRef]
63. Liu, K.; Gao, Y.; Zhu, C.; Li, K.; Fei, M.; Peng, C.; Zhang, X.; Han, Q.-L. Electrochemical modeling and parameterization towards control-oriented management of lithium-ion batteries. *Control Eng. Pract.* **2022**, *124*, 105176. [CrossRef]
64. Xie, N.; Zhao, W.; Lin, W.; Chen, Y.; Wang, Z.; Xuan, Y. A Method for Measuring Electrochemical Impedance Spectroscopy in High-voltage Battery Systems. In Proceedings of the 2024 International Conference on Energy and Electrical Engineering (EEE), Nanchang, China, 5–6 July 2024; pp. 1–5.
65. Chen, M.; Rincon-Mora, G.A. Accurate electrical battery model capable of predicting runtime and IV performance. *IEEE Trans. Energy Convers.* **2006**, *21*, 504–511. [CrossRef]
66. Wall, R.W. Simple methods for detecting zero crossing. In Proceedings of the IECON'03. 29th Annual Conference of the IEEE Industrial Electronics Society (IEEE Cat. No.03CH37468), Roanoke, VA, USA, 2–6 November 2003.
67. Syed Adil, S.; Sekyung, H. Equivalent Circuit Model Parameters Fitting Using Particle Swarm Optimization. In Proceedings of the 51st Korean Institute of Electrical Engineers Summer Conference, Busan, Republic of Korea, 15–17 July 2020.
68. Hariharan, K.S.; Senthil Kumar, V. A nonlinear equivalent circuit model for lithium ion cells. *J. Power Sources* **2013**, *222*, 210–217. [CrossRef]
69. Pierce, R.; Stacey, K.; Bardini, C. Linear functions: Teaching strategies and students' conceptions associated with y= mx+ c. *Pedagog. Int. J.* **2010**, *5*, 202–215. [CrossRef]
70. Sangwan, V.; Kumar, R.; Rathore, A.K. Estimation of battery parameters of the equivalent circuit model using Grey Wolf Optimization. In Proceedings of the 2016 IEEE 6th International Conference on Power Systems (ICPS), New Delhi, India, 4–6 March 2016; pp. 1–6.

Disclaimer/Publisher's Note: The statements, opinions and data contained in all publications are solely those of the individual author(s) and contributor(s) and not of MDPI and/or the editor(s). MDPI and/or the editor(s) disclaim responsibility for any injury to people or property resulting from any ideas, methods, instructions or products referred to in the content.